REPORT DOCUMENTATION PAGE

Form Approved
OMB No. 0704-0188

1. REPORT DATE *(DD-MM-YYYY)*	**2. REPORT TYPE**	**3. DATES COVERED** *(From - To)*
04-08-2010	Journal Article	

4. TITLE AND SUBTITLE

A Model of an Ideal Electrohydrodynamic Thruster (Preprint)

5a. CONTRACT NUMBER

5b. GRANT NUMBER

5c. PROGRAM ELEMENT NUMBER

6. AUTHOR(S)
Leonid Pekker (ERC); Marcus Young (AFRL/RZSA)

5d. PROJECT NUMBER

5f. WORK UNIT NUMBER
50260542

7. PERFORMING ORGANIZATION NAME(S) AND ADDRESS(ES)

Air Force Research Laboratory (AFMC)
AFRL/RZSA
10 E. Saturn Blvd.
Edwards AFB CA 93524-7680

8. PERFORMING ORGANIZATION REPORT NUMBER

AFRL-RZ-ED-JA-2010-349

9. SPONSORING / MONITORING AGENCY NAME(S) AND ADDRESS(ES)

Air Force Research Laboratory (AFMC)
AFRL/RZS
5 Pollux Drive
Edwards AFB CA 93524-7048

10. SPONSOR/MONITOR'S ACRONYM(S)

11. SPONSOR/MONITOR'S NUMBER(S)
AFRL-RZ-ED-JA-2010-349

12. DISTRIBUTION / AVAILABILITY STATEMENT

Approved for public release; distribution unlimited (PA #10392).

13. SUPPLEMENTARY NOTES
For publication in the Journal of Propulsion and Power.

14. ABSTRACT

We theoretically examine the idea of using the Electrohydrodynamic (EHD) ionic wind pump effect in thruster applications. This idea has been under discussion for many decades. However, there is still no commonly accepted view on EHD-thrusters, e.g., whether EHD-thruster is worthwhile or not, what level of thrust and thrust efficiency can be obtained from EHD-thrusters, etc. In this paper we present a simple one-dimensional model of an ideal EHD-thruster for calculating thrust efficiency and thrust of EHD-thrusters. We also calculate the maximum current that can be achieved for an ideal EHD-thruster at a given voltage. This allows us to calculate the maximum thrust that can be obtained from the thruster and the corresponding thrust efficiency. We show that with an increase in the voltage, the maximum trust and the corresponding thrust efficiency move in opposite directions: the thrust efficiency decreases, while the thrust increases. Our model illuminates the physical limitations of EHD-thrusters and provides reasonable estimates of the performance of real EHD-thrusters.

15. SUBJECT TERMS

16. SECURITY CLASSIFICATION OF:			**17. LIMITATION OF ABSTRACT**	**18. NUMBER OF PAGES**	**19a. NAME OF RESPONSIBLE PERSON**
					Mr. Marcus Young
a. REPORT	**b. ABSTRACT**	**c. THIS PAGE**			**19b. TELEPHONE NUMBER** *(include area code)*
Unclassified	**Unclassified**	**Unclassified**	SAR	17	N/A

Standard Form 298 (Rev. 8-98)
Prescribed by ANSI Std. 239.18

A Model of an Ideal Electrohydrodynamic Thruster (Preprint)

L. Pekker*
ERC Inc., Edwards AFB, CA 93524, USA

and

M. Young†
AFRL Edwards AFB, CA 93524, USA

We theoretically examine the idea of using the Electrohydrodynamic (EHD) ionic wind pump effect in thruster applications. This idea has been under discussion for many decades. However, there is still no commonly accepted view on EHD-thrusters, e.g., whether EHD-thruster is worthwhile or not, what level of thrust and thrust efficiency can be obtained from EHD-thrusters, etc. In this paper we present a simple one-dimensional model of an ideal EHD-thruster for calculating thrust efficiency and thrust of EHD-thrusters. We also calculate the maximum current that can be achieved for an ideal EHD-thruster at a given voltage. This allows us to calculate the maximum thrust that can be obtained from the thruster and the corresponding thrust efficiency. We show that with an increase in the voltage, the maximum trust and the corresponding thrust efficiency move in opposite directions: the thrust efficiency decreases, while the thrust increases. Our model illuminates the physical limitations of EHD-thrusters and provides reasonable estimates of the performance of real EHD-thrusters.

Nomenclature

A, B = calculated constants
E = magnitude of electrical field
E_0 = magnitude of electrical field at the anode
e = electron charge
H = altitude above sea level
i = index corresponding to i-th spatial step
j = electrical current density
$j_{\max}$ = maximum space-charge-limited current
L = the discharge length of the thruster
m_a = mass of neutral gas molecule
m_i = mass of an ion
n_a = neutral gas number density
$n_{a,0}$ = neutral gas number density at the anode
n_i = ion number density
P = gas pressure
T = thrust per unit area of the discharge
T_a = temperature of neutral gas flow
T_i = ion temperature

* Senior Research Staff Engineer, leonid.pekker.ctr@edwards.af.mil
† Manager of Advance Propulsion Group, marcus.young@edwards.af.mil

$T_{\max}$ = maximum thrust per unit area of the discharge
U = discharge voltage
U_0 = a given discharge voltage
u = velocity of neutral gas flow
u_0 = incoming velocity of neutral gas flow at the anode
u_1 = exit velocity of neutral gas flow at the cathode
V_{drift} = ion drift velocity
$V_{drift,0}$ = ion drift velocity at the anode
V_{Ta} = thermal velocity of neutral gas flow
W_k = gain of kinetic energy of gas flow per second per unit area of the discharge
W_j = electrical power deposited in the discharge per unit area of the discharge
x = axis directed along the thruster
ΔT_a = increase the gas temperature in the thruster due to Ohmic heating
ΔV = delta-V
Δx = spatial step
ε_0 = permittivity of free space
λ_{ia} = ion-neutral collision length
M_i = $\mu_i \cdot n_a$
μ_i = ion mobility
τ_{in} = ion-neutral collision time
χ = thruster efficiency

I. Introduction

Electrohydrodynamics (EHD), or alternatively electro-fluid-dynamics (EFD) or electrokinetics, refers to motion of electrically charged fluids under the influence of applied electric fields. In EHD-thrusters the applied electric field accelerates the electrically charged particles while collisional coupling between the charged particles and neutral particles is used to convert the directed energy of the charged particles into neutral gas/fluid particle flow without the need for moving parts, Fig. 1. Since the momentum transfer between ions and neutral particles is much more efficient than between electrons and neutral particles, neutral gas flows produced in EHD-devices are commonly referred to as ion wind (also ionic wind, ion-driven wind, corona wind, electric wind, and others) flows. The EHD ionic wind pump effect was discovered 1709 by Francis Hauksbee [1] and later investigated by numerous scientists including Newton, Faraday, and Maxwell; a history of EHD ionic wind pump effect can be found in excellent review of Robinson [2]. The predominantly neutral gas flows produced using the EHD pump effect have been successfully incorporated into a variety of practical devices. The most prominent application is currently ionic air purifiers such as the Ionic Breeze [3]. Such devices use the ion wind effect to drive untreated air

through the device and hit a collection plate where the unwanted particles stick to its surface. Another, more recent, application is EHD laptop cooling fans. Jewell-Larsen with his colleagues [4] have demonstrated that such devices can achieve similar cooling performance as the existing high RPM cooling fans, but at reduced noise levels. In 1961 Steutzer [5] investigated theoretically and experimentally operating the EHD ion wind devices backwards as a high voltage generator, where the ion current is generated by friction with liquid flow.

EHD based propulsion systems were proposed and investigated in the early 1960s. The most prominent effort, called the Ionocraft and led by Major de Seversky, made the front cover of Popular Mechanics in August 1964 [6]. The article described the technology as a "magic carpet" that was viable over the entire range of speeds up to and including jet aircraft speeds. It also claimed that it would become more efficient than propellers or jets for aircraft propulsion and be able to operate at altitudes as high as 60 miles. One envisioned application was an Ionocraft as large as a city block used as an antimissile platform that would indefinitely stay in the upper atmosphere. At the time of the article, however, the engineers [6] had built only a rudimentary device out of balsa wood, aluminum wire, and an electrical tether down to a high-voltage power supply. They also achieved very limited performance: it took 90W (30kV, 3mA) to lift 2oz. At that time they stated that their active work was focused on increasing the energy efficiency.

The serious theoretical and experimental investigation of EHD-thrusters began with the work of Christenson and Moller [7] in which they developed a 1D model of EHD propulsion systems and compared it with experiments. Experimentally they achieved a thruster efficiency (conversion efficiency from electrical energy to fluid kinetic energy) that was about one half of model predicted values. They concluded that approximately 90% of the input energy ended up as flow thermal energy and that the ion mobility of air would have to be reduced by about 2 orders of magnitude for realistic applications. In their theoretical analysis the authors have assumed that the ion mobility is constant and independent of gas density. Although in general, this assumption is inaccurate (it works only when $\Delta V \to 0$), their model gives reasonable estimates of the magnitude of the thrust and the trust efficiency. We also would like point out on work of Robinson [8] (which was closed to the public for a long time), where he had already in 1961 developed a very similar model as Christenson and Moller [7] for EHD-devices in which he has also included losses specific to the corona discharge. Robinson came to the same conclusion as Christenson and

Moller [7] that the conversion efficiency of EHD ion wind blowers (or EHD-thrusters) is very low. He also has pointed out that in certain gases the generation of extraneous gases in the corona discharge, e.g., ozone in air, can be a significant limitation of using corona discharge in EHD-blowers. In 1986 Bondar and Bastien [9] analytically estimated the thruster efficiency and showed that an increase of fluid velocity leads to a higher χ. They have experimentally achieved a conversion efficiency of up to 7.5% by operating with an incoming flow velocity of 50 m/s, which was close to their estimated value. In 2005 Singhal and Garimella [10] constructed a transient 3D coupled EHD/Navier-Stokes code and used it to model the effect of incoming velocity of neutral gas on efficiency of EHD-pumps (or EHD-thrusters). As Bondar and Bastien, they concluded that significant increases in conversion efficiency of EHD-pumps are possible by increasing the incoming velocity into the EHD-pumps. In recent work [11] the authors have shown that the exhaust velocity can be increased by adding multiple stages of EHD-thrusters in series. They demonstrated a maximum axial velocity for a single stage 2.5 cm diameter device of 4.5 m/s. They also tested up to 7 stages in series yielding a maximum velocity of over 7m/s, but at a conversion efficiency of around 0.1%.

Thus, the primary limitation of EHD based propulsion systems is that they are typically very inefficient in terms of thrust efficiency when operating on gases, roughly 1-10%, while competing technologies like fans can achieve χ of 60%-70% [8]. There are, however, other factors that could limit the applicability of EHD based propulsion systems. One of them is that the ion current is charge limited [7, 8] that leads to small ionization fractions in EHD thrusters, typically in the order of 10^{-10} at one Atm air pressure. This indicates that space charge built in the EHD thruster chambers may limit the amount of achievable thrust per unit area. Other factors such as local humidity and subtle electrode alignment changes greatly affected the maximum attainable ion wind velocity [11] indicating that EHD propulsion systems may not be very robust. Obviously many other factors can negatively impact the performance of EHD-thrusters. However, there is still no commonly accepted view on EHD-thruster, e.g., whether EHD-thruster is worthwhile or not, what level of thrust and thrust efficiency can be obtained from EHD-thrusters, etc. Therefore, the construction of an ideal model of EHD thrusters is very important for understanding major physical limitations of EHD thrusters in "ideal situations".

In this paper we present a simple one-dimensional model of an ideal EHD thruster. A description of the model and numerical results are presented in Section II and III, respectively, and conclusions are given in Section IV.

II. Description of the Model

A schematic of an ideal electrohydrodynamic thruster is shown in Fig. 1. The ions are "seeded" at the anode and are absorbed at the cathode. Here we do not consider the mechanism for creating the ions. They can be created, for example, by corona discharge, or by other means. The neutral gas flow is coming from the anode side of the thruster. Due to the friction forces with ions, the neutral gas flow is accelerated in the discharge thruster region that creates the thrust, as in an ordinary air turbine jet.

The following assumptions are made in the model, Fig. 1: 1) the width of the thruster is much larger than the length of the thruster L; 2) all parameters of incoming neutral gas and ion flow are uniform across the thruster; 3) the anode and the cathode are transparent for the neutral gas flow; 4) there are no electrons in the discharge region; 5) all parameters of the thruster are independent of time (i.e., we assume the steady state regime of thruster operation); 6) the temperature of neutral gas flow in the discharge chamber is constant. The sixth assumption relies on the assumption that the electrical power put into the discharge is relatively small so that the heating of the gas flow due to the discharge can be ignored. It follows from assumptions 1 – 3 that our model is one-dimensional.

The equations describing one-dimensional thrusters, Fig. 1, are

$$\varepsilon_0 \cdot \frac{dE}{dx} = -e \cdot n_i \tag{1}$$

$$j = e \cdot n_i \cdot (u + V_{drift}) = const \tag{2}$$

$$n_{a,0} \cdot u_0 = n_a \cdot u \tag{3}$$

$$m_a \cdot n_{a,0} \cdot u_0 \cdot \frac{du}{dx} = n_i \cdot e \cdot E \tag{4}$$

where Eq. (1) is Payson law, Eq. (2) is electrical charge conservation law, Eq. (3) is mass conservation law for neutral particles, and Eq. (4) is momentum conservation law for ions, and

$$V_{drift} = \mu_i \cdot E \tag{5}$$

$$\mu_i = \frac{e \cdot \tau_{in}}{m_i} = \frac{\mathrm{M}_i}{n_a} \tag{6}$$

In Eq. (2) we have assumed that the ion-neutral collision mean-free-path, is much smaller than L and, therefore, the ion velocity without the electric field has to be about equal to the local velocity of gas flow. It should be stressed that in the case where a corona discharge is used to ionize the incoming gas flow, Eq. (2) is exact. In the model we also assume that M_i is a constant. This is a reasonable assumption as long as the relative velocity between the gas flow and the ion "wind", V_{drift}, is smaller than the neutral particle thermal velocity, V_{Ta}, and the temperature of gas flow T_a does not change significantly in the discharge region of the EHD-thruster, assumption 6. It should be stressed that in the case of strong electric fields, when the energy that an ion gains from the electric field between collisions is comparable to the temperature of the neutral gas (V_{drift} calculated by Eq. (5) becomes larger than V_{Ta}), the ion drift cannot be described by Eq. (5) any longer [12]. It is worth noting that this situation corresponds, in particular, to the case of the electrical breakdown in gasses. The system of Eqs. (1) – (6) is essentially the system of equation of Christensen-Moller [7], however taking into account dependence of ion mobility on density of neutral gas.

Integrating Eq. (4) along the discharge region we obtain an equation for the thrust per unit of area of the discharge,

$$T = m_a \cdot n_{a,0} \cdot u_0 \cdot (u_1 - u_0) = e \cdot \int_0^L n_i \cdot E \cdot dx \tag{7}$$

Multiplying Eq. (4) by u and then integrating along the discharge region we obtain an equation for the gain of kinetic energy of gas flow per second per unit of area of the discharge,

$$W_k = m_a \cdot n_{a,0} \cdot u_0 \cdot \left(\frac{u_1^2}{2} - \frac{u_o^2}{2} \right) = \int_0^L n_i \cdot e \cdot E \cdot u \cdot dx \tag{8}$$

The electrical power deposited in the discharge per unit area of the discharge can be calculated as

$$W_j = j \cdot \int_0^L E \cdot dx = j \cdot U \tag{9}$$

where

$$U = \int_0^L E \cdot dx \tag{10}$$

The system of Eqs. (1) – (6) can be reduced to the following system of two ordinary differential equations,

$$\frac{dV_{drift}}{dx} = B \cdot \frac{V_{drif}^2}{(V_{drift} + u) \cdot u^2} - A \cdot \frac{u}{(V_{drift} + u)} \tag{11}$$

$$\frac{du}{dx} = B \cdot \frac{V_{drift}}{(V_{drift} + u) \cdot u} \tag{12}$$

where A and B are constants:

$$A = \frac{j \cdot \mathrm{M}_i}{\varepsilon_0 \cdot n_{a,0} \cdot u_0} \quad \text{and} \quad B = \frac{j}{\mathrm{M}_i \cdot m_a} \tag{13}$$

We have numerically solved Eqs. (11) – (13) with two boundary conditions:

$$u(x = 0) = u_0 \text{ and } U = U_0 \tag{14}$$

Now let us consider the case where the ion's drift velocity is much larger then the velocity of neutral gas flow,

$$V_{drif} >> u \tag{15}$$

Dropping u in Eq. (2), we obtain the following equation for E,

$$\varepsilon_0 \cdot \frac{dE}{dx} = -\frac{j}{\mu_i \cdot E} \tag{16}$$

Assuming further that μ_i = const and solving Eq. (16) analytically for given j and E_0, we obtain the following analytical estimates for $n_i(x)$, $E(x)$, U, and $j_{\max}$:

$$n_i = \frac{j}{e \cdot \mu_i \cdot E_0} \cdot \left(1 - \frac{x}{L} \cdot \left(\frac{j}{j_{\max}}\right)\right)^{-1/2} \tag{17}$$

$$E = E_0 \cdot \left(1 - \frac{x}{L} \cdot \left(\frac{j}{j_{\max}}\right)\right)^{1/2} \tag{18}$$

$$U = \frac{2}{3} \cdot E_0 \cdot L \cdot \frac{j_{\max}}{j} \cdot \left(1 - \left(1 - \frac{j}{j_{\max}}\right)^{3/2}\right) \tag{19}$$

where

$$j_{\max} = \frac{\varepsilon_0 \cdot \mu_i \cdot E_0^2}{2 \cdot L} = \frac{9 \cdot \varepsilon_0 \cdot \mu_i \cdot U^2}{8 \cdot L^3} \tag{20}$$

It follows from Eq. (17) that the current cannot exceed the maximum space-charge-limited current $j_{\max}$, the Child-Langmuir Law. In the case when $j \to 0$ we obtain that $U = E_0 \cdot L$ and $n_i = 0$, and when $j = j_{\max}$ Eq. (19) yields $U = \frac{2}{3} \cdot E_0 \cdot L$. Substituting Eq. (17) – (19) into Eqs. (7) and (8) and setting u to u_0 in the right-hand-side of Eq. (8) we obtain analytical estimates for the thrust and the thrust efficiency,

$$T \approx \frac{j \cdot L}{\mu_i} \tag{21}$$

$$\chi = \frac{W_k}{W_j} \approx \frac{u \cdot L}{\mu_i \cdot U} \approx \frac{u}{V_{drift}} \tag{22}$$

Substituting $j_{\max}$, Eq. (20), into Eq. (21) we obtain an estimate for the maximum thrust that can be achieved from the thruster,

$$T_{\max} \approx \frac{j_{\max} \cdot L}{\mu_i} = \frac{9 \cdot \varepsilon_0 \cdot U^2}{8 \cdot L^2} \tag{23}$$

As one can see from Eq. (23), the maximum thrust is independent of ion mobility when $V_{drif} \gg u$. It follows from Eqs. (22) and (23) that with an increase in the thruster voltage, $T_{\max}$ increases while χ decreases. This shows that achieving both targets, high thrust and high thrust efficiency, at once can be difficult.

III. Numerical results

The exact calculation of ion drift mobility in air is a very complicated task; notably it depends on ion composition, humidity of air, pressure, and other factors. Direct measurements of average natural air ion mobility at one atmosphere [13] give $\mu_i \approx 1.39 \cdot 10^{-4}$ m^2/(V·sec) with a standard deviation of $0.1 \cdot 10^{-4}$ m^2/(V·sec). Since, the ion mobility of N_2^+ in pure nitrogen gas at a pressure of one atmosphere and a temperature of 300 K is $1.37 \cdot 10^{-4}$ m^2/(V·sec) [12] and close to the measured average natural ion mobility

of air, we consider in our paper the case of pure nitrogen gas. In our calculations we have used $\mathrm{M}_i = 1.27 \cdot 10^{24}$ [V/(sec·m)] that corresponds to drift of ions N_2^+ in nitrogen gas at gas temperature of 300K. Since M_i is weakly dependent on the temperature ($\mathrm{M}_i = 1.01 \cdot 10^{24}$ m^2/(V·sec) at 1000 K), our assumption that M_i = const is well satisfied.

Figs. 2 - 13 present the result obtained by numerically solving the system of Eqs. (11) – (14) at maximum current (maximum thrust). Fig. 2 shows maximal current densities vs. voltage for different velocities of neutral gas flow u_0; in our model u_0 can be interpreted as the speed of the vehicle. As it has been expected with an increase in applied voltage, $j_{\max}$ increases rapidly. As shown in Fig. 3 the maximum thrust of the EHD-thruster increases with an increase in the voltage (as expected) and seems not to depend greatly on the speed of vehicle as in the case of $V_{drift} >> u$, Eq. (23). Fig. 4 shows that thruster efficiency increases with an increase in the speed of the vehicle and decreases with an increase in the applied voltage; these trends agree with an estimate of χ for the case of $V_{drift} >> u$, Eq. (22) and qualitatively agree with the Bondar-Bastein model [9].

To investigate how the length of EHD-thruster affects the thruster performance we have calculated parameters of the EHD thruster for $u_0 = 50$ m/s and $L = 1$ m for different $j_{\max}$, Figs. 5 – 10. As shown in Fig. 5 the discharge voltage increases very non-linearly with the length of the capillary for fixed magnitude of $j_{\max}$. This behavior of U vs. L can be explained by significant non-linear dependencies of the electric field on discharge for currents close to $j_{\max}$; see an analytical expression for U in Eq. (20) for the case of $V_{drift} >> u$. With an increase in L the thrust increases more or less linearly, Fig. 6, but, the thrust efficiency decreases sharply, Fig. 7. We have also calculated ΔV, one of the important parameters of thruster performance, Fig. 8. As one can see ΔV reaches about 4.5 m/s for $L = 100$ cm and $j_{\max} = 0.05$ A/m^2. Since the ion current cannot exceed the space-charge-limited current $j_{\max}$, the ion density in the discharge is very small, Fig. 9.

To investigate the performance of the thruster at different altitudes we have also calculated the thrust and thruster efficiency for H = 20 km. As shown in Figs. 10 and 11, both thrust and thrust efficiency decrease with an increase in H. The reason is that ion mobility increases with a decrease in gas density,

Eq. (6), leading to a decrease in $T_{\max}$ and χ ($T_{\max} \propto \mu_i^{-1}$ and $\chi \propto \mu_i^{-1/2}$, Eqs. (22) and (23)). Thus, since the drag and the thrust are approximately proportional to gas pressure, using EHD-thrusters at high altitudes does not make much sense.

To investigate to what extent the simple analytical Eqs. (22) and (23) are applicable, we have calculated the ratios of analytically predicted thrust and thruster efficiency to numerically calculated $T_{\max}$ and χ, Figs. 12 and 13 respectively. Fig. 13 also shows the Bondar-Bastein estimated thruster efficiency [9],

$$\chi = \frac{u_0}{u_0 + \dfrac{\mu_i \cdot U}{L}} \tag{24}$$

which coincides with Eq. (22) when $V_{drift} >> u$. As one can see Eqs. (23) and (24) give reasonable estimates for the $T_{\max}$ and χ in almost all regions of $j_{\max}$, while Eq. (22) works only for large $j_{\max}$ corresponding to large V_{drift}.

The increase in temperature of gas flow due to Ohmic heating by the discharge can be estimated as

$$\Delta T_a \approx \frac{2 \cdot (W_j - W_k - n_i \cdot V_{drift}^3)}{3 \cdot k \cdot n_a \cdot u_0} \tag{25}$$

As shown in Fig. 14 , ΔT_a increases with a decrease in speed of the vehicle and with an increase in the length of the thruster; this makes perfect sense. The faster neutral gas streams through the EHD-discharge chamber, the smaller ΔT_a gets. Since ΔT_a is quite small even for L = 1m, the sixth assumption in Section II is well satisfied.

Table. 1 shows the ratio of the ion drift velocity at the anode (where electrical field is largest) to the thermal velocity of neutral gas flow and $U/(P \cdot L)$ for different altitudes, gas flow velocities, and lengths of the EHD-thruster. As was mentioned in Section II, when V_{drift}/V_{Ta} approaches unity, Eq. (5) for ion mobility becomes invalid. Since the electrical breakdown voltage of nitrogen gas is about $1.4 \cdot 10^6$ V/(m·Atm) [12] (and is close to the electrical breakdown of air [14]), the electrical breakdown most likely appears before Eq. (5) became invalid, Table 1. Therefore, the obtained results in the case when $V_{drift}/V_{Ta} > 1$ should be considered from an illustrative point of view only.

IV. Conclusions

We presented a one-dimensional model of an ideal EHD-thruster. We showed that the ion current in an ideal EHD-thruster has a principal limit; it cannot exceed the space-charge-limited current $j_{\max}$, and therefore, the thrust of such a thruster cannot exceed the thrust corresponding to this current. We also show that thrust and thrust efficiency "work" against each other in EHD-thrusters: the larger the thruster current (larger thrust) the smaller the thruster efficiency. We also show that at high altitudes the performance of EHD-thrusters (thrust and thrust efficiency) drops very fast, and therefore, using EHD-thrusters at altitudes larger than 5 km is apparently unrealistic. The model shows that maximum thrust cannot exceed 20 – 30 N/m^2 at sea level even at breakdown voltage; thus, this also does not look very encouraging. Since our model is an ideal and does not take into account numerous other factors that can negatively impact the performance of EHD-thrusters even more, we may conclude that the idea of using the Electrohydrodynamic ionic wind pump effect for thruster application is rather dim.

References

[1] Hauksbee, F., "Physico-Mechanical Experiments on Various Subjects," London, 1709, 1st Edition, pp. 46-47.

[2] Robinson, M., "A History of the Electric Wind," American Journal of Physics, Vol. 30, No. 5, 1960, pp. 366-372.

[3] Rickard, M., Dunn-Rankin, D., Weinberg, F., Carleton, F., "Characterization of Ionic Wind Velocity," Journal of Electrostatics, Vol. 63, 2005, pp. 711-716.

[4] Jewell-Larsen, N., E., Ran, H., Zhang, Y., Schweibert, M., Honer, K., A., "Electrohydrodynamic (EHD) Cooled Laptop," 25th IEEE SEMI-THERM Symposium, San Jose, CA, March 15-19, 2009.

[5] Stuetzer, O. M., "Ion Transport High Voltage Generators," The Review of Scientific Instruments, Vol. 32, 1961, pp. 16-22.

[6] Fentei, H., "Major de Seversky's Ion -Propelled Aircraft," Popular Mechanics, Aug. 1964, 58-196.

[7] Christenson E. A., and Moller P.S., “Ion-Neutral Propulsion in Atmosphere Media,” AIAA Journal, Vol. 5, No. 5, 1967, pp. 1768-1773.

[8] Robinson, M., "Movement of Air in the Electric Wind of the Corona Discharge," ASTIA Document AD-262A30, 1961.

[9] Bondar, H. and Bastein, F., “Effect of neutral fluid velocity on direct conversion from electric to fluid kinetic energy in an electro-fluid-dynamic (EFD) device,” J. Phys. D: Appl. Phys., Vol. 19, 1986, pp. 1657-1663.

[10] Singhal, V., Garimella, S. V., "Influence of Bulk Fluid Velocity on the Efficiency of Electrohydrodynamic Pumping,” Transactions of the ASME, Vol. 127, 2005 pp. 484-494.

[11] Rickard, M., Dunn-Rankin, D., Weinberg, F., Carleton, F., "Maximizing ion-driven gas flows,” Journal of Electrostatics, 64, pp. 368-376, (2006).

[12] Raizer, Y. P., “Gas Discharge Physics,” Springer, New York, 1997.

[13] Tammet, H., Iher H., and Salm, J., “Spectrum of Atmosphere Ions in the Mobility Range of 0.32 – 3.2 $cm^2/(V\circ s)$,” Acta et Comm.Univ. Tartuensis, Vol. 947, 1992, pp. 35-49.

[14] Akamine, V., Matsuoka, S., Chiba, M., Hidaka, K., “Electrical Breakdown Characteristics of Nitrogen and Air at Cryogenic Temperatures in Quasi-Uniform Electric Field,” Electric Engineering in Japan, Vol. 132, No 4, 2000, pp. 28-33.

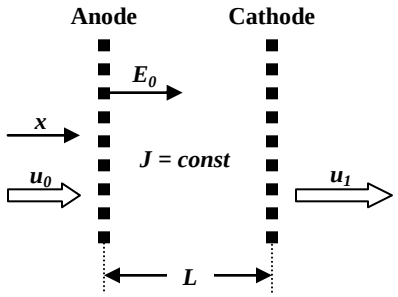

Fig. 1. Schematic (not to scale) of electrohydrodynamic thruster.

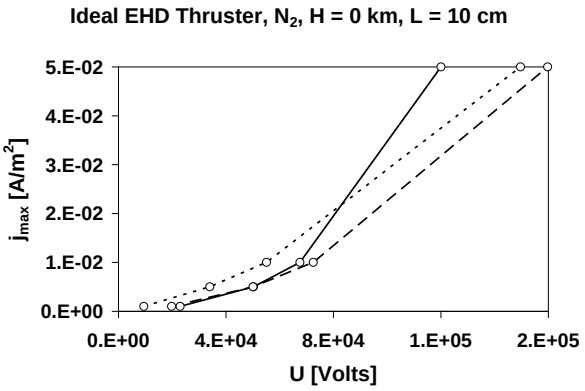

Fig. 2. Maximum current; solid line: u_0 = 3 m/s, dashed line: u_0 = 10 m/s, dotted line: u_0 = 50 m/s.

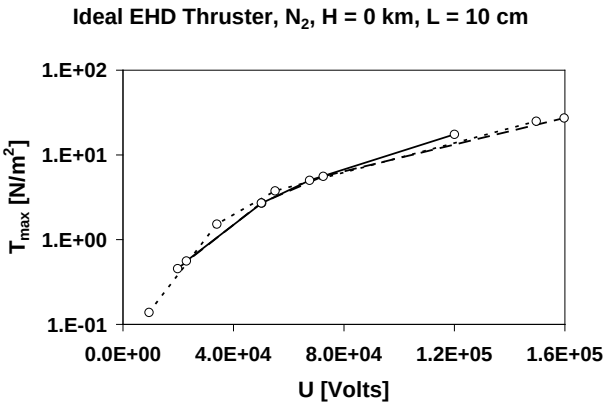

Fig. 3. Thrust at maximum current; solid line: u_0 = 3 m/s, dashed line: u_0 = 10 m/s, dotted line: u_0 = 50 m/s.

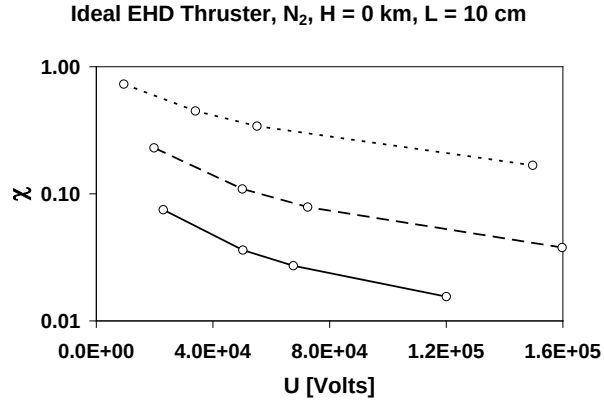

Fig. 4. Thrust efficiency at maximum current; solid line: u_0 = 3 m/s, dashed line: u_0 = 10 m/s, dotted line: u_0 = 50 m/s.

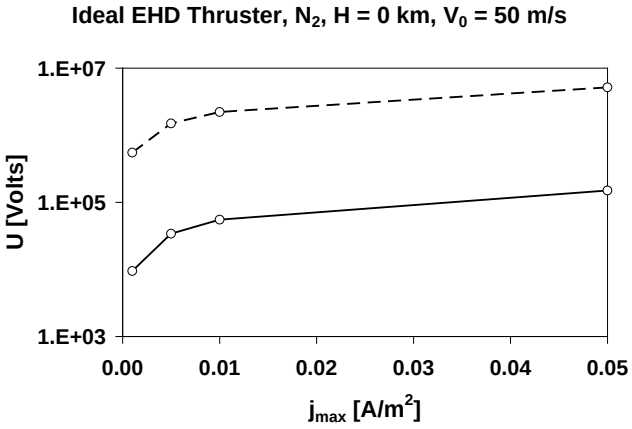

Fig. 5. Voltage at maximum current; solid line: L = 10 cm, dashed line: L = 100 cm/s.

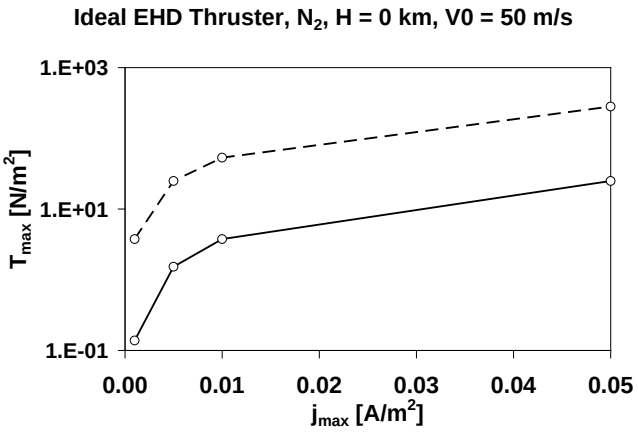

Fig. 6. Thrust at maximum current; solid line: L = 10 cm, dashed line: L = 100 cm/s.

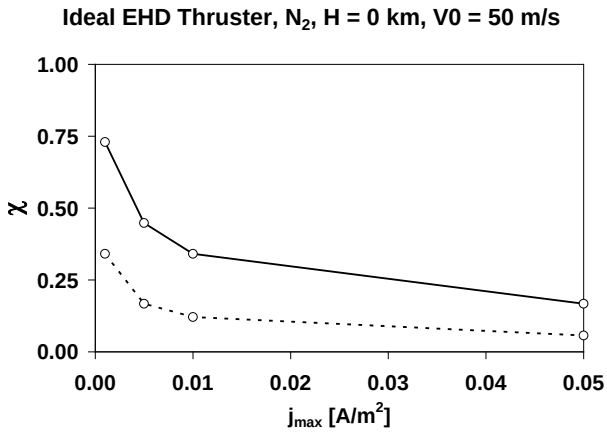

Fig. 7. Thrust efficiency at maximum current; solid line: L = 10 cm, dashed line: L = 100 cm/s.

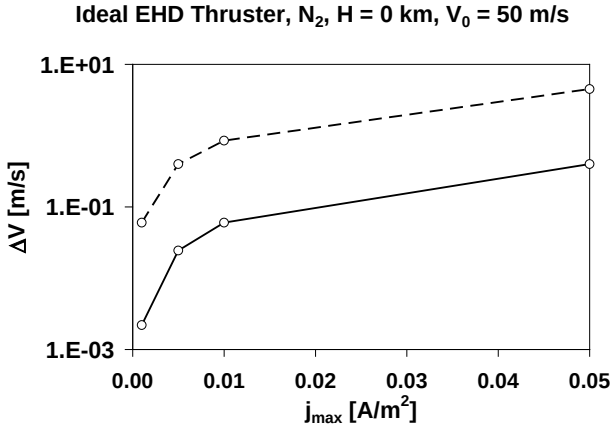

Fig. 8. Delta-V at maximum current; solid line: L = 10 cm, dashed line: L = 100 cm/s.

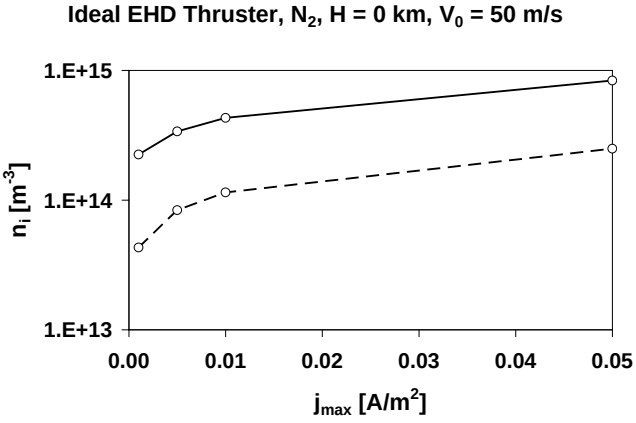

Fig. 9. Ion density at maximum current; solid line: L = 10 cm, dashed line: L = 100 cm/s.

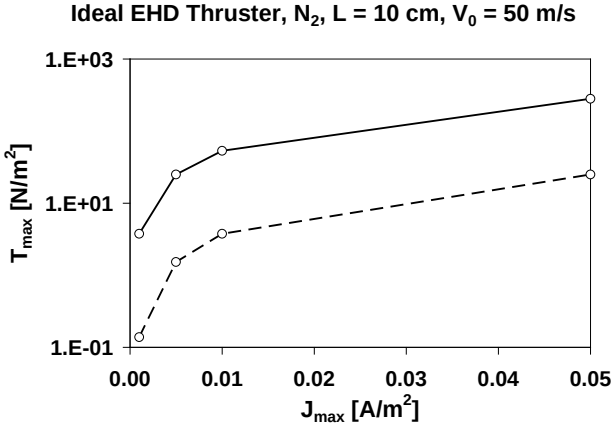

Fig. 10. Thrust at maximum current; solid line: H = 0 km, dashed line: H = 20 km.

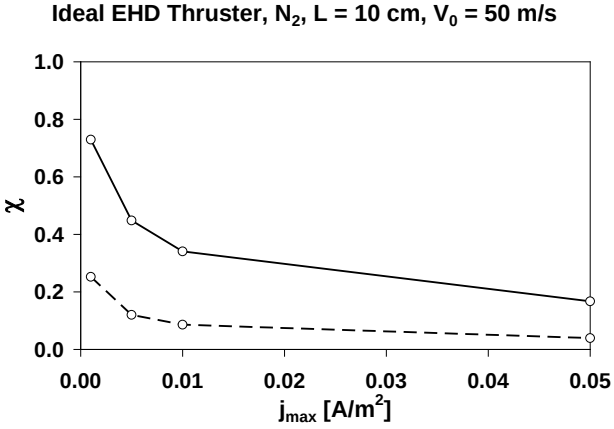

Fig. 11. Thrust efficiency at maximum current; solid line: H = 0 km, dashed line: H = 20 km.

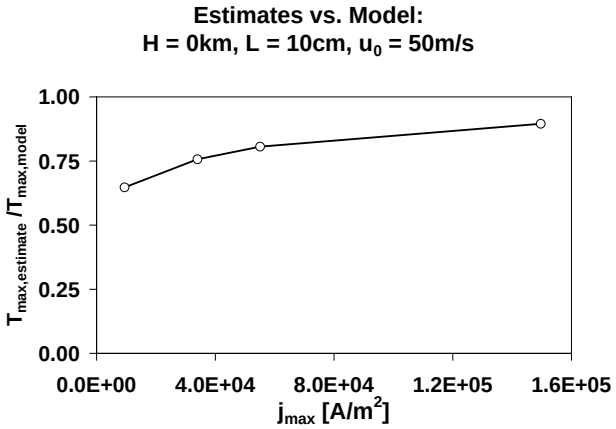

Fig. 12. Ratio of the estimated thrust to the numerically calculated thrust at maximum current.

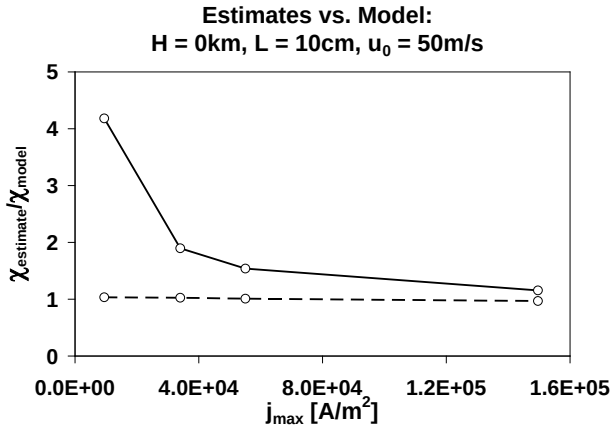

Fig. 13. Ratio of the estimated thrust efficiency to the numerically calculated thrust at maximum current; solid line: Eq (22), dashed line: Eq. (24).

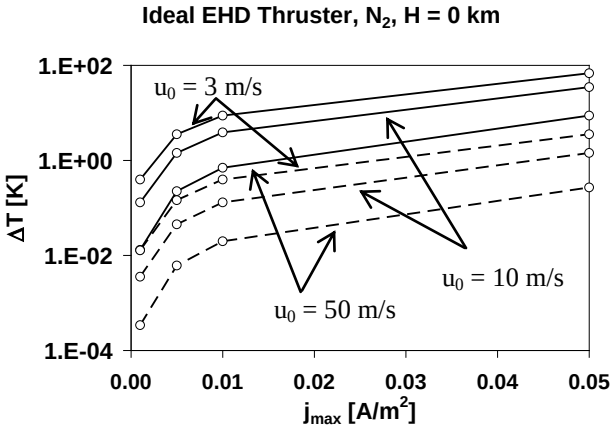

Fig. 14. An estimation for ΔT_a ; solid lines: L = 1m, dashed lines L = 10cm

Table 1. V_{drift}/V_{Ta} **and** E/P **[Volts/(m·Atm)]**

					$H = 20km$ $L = 0.1m$
$H = 0km$ $L = 0.1m$			$L = 1m$		
$V_0 = 3m/s$	$V_0 = 10m/s$	$V_0 = 50m/s$	$V_0 = 50m/s$		$V_0 = 50m/s$

A/m^2	V_{drift}/V_{Ta}	E/P	V_{drift}/V_{Ta}	E/P	V_{drift}/V_{Ta}	E/P	V_{drift}/V_{Ta}	E/P	V_{drift}/V_{Ta}	E/P
0.001	0.07	$8.63x10^4$	0.12	$1.80x10^5$	0.13	$2.09x10^5$	0.34	$5.02x10^5$	0.61	$7.85x10^5$
0.005	0.022	$3.10x10^5$	0.29	$4.56x10^5$	0.29	$4.58x10^5$	0.89	$1.36x10^6$	1,53	$2.04x10^6$
0.01	0.34	$5.02x10^5$	0.42	$6.06x10^5$	0.40	$6.15x10^5$	1.29	$2.02x10^6$	2.22	$2.98x10^6$
0.05	0.89	$1.36x10^6$	0.92	$1.45x10^6$	0.74	$1.09x10^6$	2.97	$4.70x10^6$	5.12	$6.99x10^6$